# Delft University of Technology

## Sensor Selection for Angle of Arrival Estimation Based on the Two-Target Cramér-Rao Bound

Kokke, Costas A.; Coutino, Mario; Anitori, Laura; Heusdens, Richard; Leus, Geert

**Citation (APA)**
Kokke, C. A., Coutino, M., Anitori, L., Heusdens, R., & Leus, G. (2023). Sensor Selection for Angle of Arrival Estimation Based on the Two-Target Cramér-Rao Bound. In *Proceedings of the ICASSP 2023 - 2023 IEEE International Conference on Acoustics, Speech and Signal Processing (ICASSP)* (ICASSP, IEEE International Conference on Acoustics, Speech and Signal Processing - Proceedings; Vol. 2023-June). IEEE. https://doi.org/10.1109/ICASSP49357.2023.10094942

**Important note**
To cite this publication, please use the final published version (if applicable).
Please check the document version above.

# SENSOR SELECTION FOR ANGLE OF ARRIVAL ESTIMATION BASED ON THE TWO-TARGET CRAMÉR-RAO BOUND

*Costas A. Kokke*[‡]*, Mario Coutino*[⋆]*, Laura Anitori*[⋆]*, Richard Heusdens*[†]*, Geert Leus*[‡]

[⋆]Netherlands Organisation for Applied Scientific Research, The Hague, The Netherlands
[†]Netherlands Defence Academy, Den Helder, The Netherlands
[‡]Delft University of Technology, Delft, The Netherlands

## ABSTRACT

Sensor selection is a useful method to help reduce data throughput, as well as computational, power, and hardware requirements, while still maintaining acceptable performance. Although minimizing the Cramér-Rao bound has been adopted previously for sparse sensing, it did not consider multiple targets and unknown source models. In this work, we propose to tackle the sensor selection problem for angle of arrival estimation using the worst-case Cramér-Rao bound of two uncorrelated sources. To do so, we cast the problem as a convex semi-definite program and retrieve the binary selection by randomized rounding. Through numerical examples related to a linear array, we illustrate the proposed method and show that it leads to the natural selection of elements at the edges plus the center of the linear array. This contrasts with the typical solutions obtained from minimizing the single-target Cramér-Rao bound.

***Index Terms***— sparse sensing, cramér-rao bound, multi-target estimation, array processing, sensor selection

## 1. INTRODUCTION

Among the main functions of a radar system is angle of arrival (AoA) estimation. In modern radar, antenna arrays are used to realize the acquisition of spatial data and the application of beamforming. The aperture of the array is the primary contributor to the angular resolution of the array, while the density of the array allows further suppression outside the main beam and prevention of spatial aliasing.

So naturally, a large aperture, densely packed array should be desirable, but it should come as no surprise that this carries a cost. The need for more hardware (both antennas and their processing) leads to a higher cost, but it also leads to a large amount of data. Not only would we need the computing power to process all the data, we also need the throughput to actually get all the data to the processor. Further, the additional hardware and processing also incur an additional power cost.

Since the ratio of targets to obtained sensors is usually low, compressed sensing (CS) has been shown to be effective at reducing the required data processing while maintaining performance [1, 2, 3]. However, even though CS can be implemented using analog processing with low-complexity receiver chains, the entire array still need to be available. To mitigate the hardware costs, we need to design arrays that are sparse, i.e., perform sensor selection.

Sensor selection is the problem of choosing a subset of sensors from a full set of candidate sensors, e.g., a uniform linear array (ULA). It can be performed both offline, in the design of the array, or online, by switching between the available elements of the array. Offline sensor selection carries the biggest cost savings, clearly, but there is no option to adapt the sensor selection to a specific task or scenario. Online sensor selection has the ability to adapt to different tasks and scenarios, but requires all candidate sensors to be available as well as a switching mechanism, both of which directly lead to increased costs. In this work, we will focus on offline sensor selection through convex optimization, though in Section 6 we will discuss some possible extensions to online sensor selection.

Convex optimization has previously been used successfully in sensor selection, such as by relaxing a non-convex program [4, 5, 6] to a convex one. Casting the problem as a convex optimization problem has the obvious benefits of guarantees regarding the optimum, and efficient and well-studied optimization methods. We will see that our proposed model and metric allow for an equivalent mixed-integer convex program to solve the sensor selection problem.

To perform the sensor selection, a metric to evaluate the quality of selection is required. The Cramér-Rao bound (CRB) is a natural choice, especially for offline sensor selection, since it can be used to quantify estimation performance independent of the estimation method used. The CRB has previously been used successfully for sensor selection in [7, 8, 9]. Previous work has not yet considered the case of multiple unknown sources however, which is what we propose in this work.

In Section 2 we present the signal model, its associated multi-target CRB and discuss the specific selection that we would like to find using our method. The proposed method is presented in Section 4, where we also show the derivations to obtain the final convex semidefinite program. We present the results of our simulations as verification of our proposed method in Section 5 and we conclude in Section 6 with some discussion.

## 2. SIGNAL MODEL

Let the received data for a $K$-target, $N$-element array over $T$ temporal samples be given by

$$\boldsymbol{X} = \boldsymbol{A}(\boldsymbol{\omega})\boldsymbol{S}^{\mathrm{T}} + \boldsymbol{E} \in \mathbb{C}^{N \times T}, \tag{1}$$

where $\boldsymbol{A}(\boldsymbol{\omega}) = \begin{bmatrix} \boldsymbol{a}(\omega_1) & \cdots & \boldsymbol{a}(\omega_K) \end{bmatrix} \in \mathbb{C}^{N \times K}$ is a matrix containing the array response of each target as its columns, $\boldsymbol{\omega} \in \mathbb{R}^K$ is the vector containing the target AoAs, and $\boldsymbol{E}$ is additive noise. $\boldsymbol{S} = \begin{bmatrix} \boldsymbol{s}_1 & \cdots & \boldsymbol{s}_K \end{bmatrix} \in \mathbb{C}^{T \times K}$ is a matrix containing the target signals. The columns of $\boldsymbol{S}$ consist of the, potentially different, transmit waveform(s) reflected by a number of targets, where every target

can be characterized by a different delay, radial velocity and reflection coefficient. We further assume the noise captured in $\boldsymbol{E}$ to be zero-mean complex Gaussian distributed, and spatially and temporally uncorrelated with variance $\sigma_e^2$.

For the above model, the CRB for $\boldsymbol{\omega}$, assuming $\boldsymbol{S}$ is a deterministic nuisance, is given by [10]

$$\mathrm{CRB}(\boldsymbol{\omega}) = \frac{\sigma_e^2}{2T}\Big(\mathrm{Re}\Big\{\boldsymbol{D}^{\mathrm{H}}\boldsymbol{D}\circ\boldsymbol{R}^{\mathrm{T}} \\ - \boldsymbol{D}^{\mathrm{H}}\boldsymbol{A}\big(\boldsymbol{A}^{\mathrm{H}}\boldsymbol{A}\big)^{-1}\boldsymbol{A}^{\mathrm{H}}\boldsymbol{D}\circ\boldsymbol{R}^{\mathrm{T}}\Big\}\Big)^{-1}, \quad (2)$$

where "$\circ$" indicates the Hadamard product, $\boldsymbol{R} = \frac{1}{T}\boldsymbol{S}^{\mathrm{T}}\boldsymbol{S}$ takes the cross-correlation between the different source signals and can be viewed as a sample covariance matrix, and

$$\boldsymbol{D} = \begin{bmatrix}\boldsymbol{d}(\omega_1) & \cdots & \boldsymbol{d}(\omega_K)\end{bmatrix} \\ = \begin{bmatrix}\frac{\partial \boldsymbol{a}(\omega_1)}{\partial \omega_1} & \cdots & \frac{\partial \boldsymbol{a}(\omega_K)}{\partial \omega_K}\end{bmatrix} \in \mathbb{C}^{N\times K}.$$

In the single-target case, this simplifies to

$$\mathrm{CRB}_1 = \frac{\sigma_e^2}{2T\sigma_s^2}\Big(\mathrm{Re}\Big\{\boldsymbol{d}^{\mathrm{H}}\Big(\boldsymbol{I} - \boldsymbol{a}\big(\boldsymbol{a}^{\mathrm{H}}\boldsymbol{a}\big)^{-1}\boldsymbol{a}^{\mathrm{H}}\Big)\boldsymbol{d}\Big\}\Big)^{-1}, \quad (3)$$

where $\sigma_s^2 = \frac{1}{T}\boldsymbol{s}^{\mathrm{T}}\boldsymbol{s}$. Conveniently, this expression can be shown to be independent of the variable $\omega_1$. In (2), we do not get this independence unfortunately, due to the different sources acting as nuisances influencing each other. However, the primary reason to optimize the antenna positions using the multi-target CRB as opposed to the single-target CRB in (3), is that in the single-target case additional constraints are needed to suppress sidelobes in the beampattern response to an acceptable level for multi-target operation [8]. By optimizing a multi-target objective, the need for such additional constraints should be alleviated.

In many AoA problems, the columns of $\boldsymbol{S}$ can be considered uncorrelated. For instance in passive radar, we may assume that the targets reflect unrelated and hence uncorrelated signals. Additionally, we expect changes in the target reflectors due to movement, making the reflected signals uncorrelated. If we further assume for the sake of simplicity and clarity that $T$ is large and the sources have the same unit power, then we obtain $\boldsymbol{R} = \boldsymbol{I}$. Although such an assumption may seem restrictive, extensions to sources with different powers or other correlation patterns are possible as we will discuss briefly in Section 6.

## 3. PROBLEM FORMULATION

Although the antenna positions could be directly optimized from the CRB (i.e. [11]), we follow a sensor selection approach here. To formalize this, we assume that the data model in (1) is based on a uniform linear array (ULA) of $N$ antennas from which we select $M$ antennas through a selection vector $\boldsymbol{p} \in \{0,1\}^N$, where a one indicates that the related antenna is selected, and a zero means it is not. Since $M$ antennas need to be selected we have $\boldsymbol{1}^{\mathrm{T}}\boldsymbol{p} = M$. The sample selection can be written as $\boldsymbol{y} = \boldsymbol{\Phi}(\boldsymbol{p})\boldsymbol{x}$ where $\boldsymbol{\Phi}(\boldsymbol{p}) \in \{0,1\}^{M\times N}$ is a binary selection matrix constructed by removing the all-zero rows from $\boldsymbol{P} = \mathrm{diag}(\boldsymbol{p})$, so $\boldsymbol{\Phi}(\boldsymbol{p})\boldsymbol{\Phi}^{\mathrm{T}}(\boldsymbol{p}) = \boldsymbol{I}_M$ and $\boldsymbol{\Phi}^{\mathrm{T}}(\boldsymbol{p})\boldsymbol{\Phi}(\boldsymbol{p}) = \boldsymbol{P}$.

The task of our sensor selection approach for AoA estimation now aims to find a selection vector $\boldsymbol{p}$, which performs better in multi-target AoA estimation than any other selection of $M$ out of $N$ antennas, i.e.,

$$\min_{\boldsymbol{p}\in\{0,1\}^N} f(\boldsymbol{p}) \quad \text{s.t. } \boldsymbol{1}^{\mathrm{T}}\boldsymbol{p} = M, \quad (4)$$

where $f(\boldsymbol{p})$ is the chosen metric as function of the selection vector. To tackle this problem, we propose to quantify the performance of the selection vector using the multi-target CRB [cf. (2)] yet of the subarray consisting of the selected sensors. This CRB can be obtained by replacing in (2), $\boldsymbol{A}$ and $\boldsymbol{D}$ respectively by $\boldsymbol{\Phi}(\boldsymbol{p})\boldsymbol{A}$ and $\boldsymbol{\Phi}(\boldsymbol{p})\boldsymbol{D}$. Finally, setting $\boldsymbol{R} = \boldsymbol{I}$ as discussed earlier, we obtain

$$\mathrm{CRB}(\boldsymbol{\omega},\boldsymbol{p}) = \frac{\sigma^2}{2T}\Big(\mathrm{Re}\Big\{\boldsymbol{D}^{\mathrm{H}}\boldsymbol{P}\boldsymbol{D}\circ\boldsymbol{I} \qquad (5) \\ - \boldsymbol{D}^{\mathrm{H}}\boldsymbol{P}\boldsymbol{A}\big(\boldsymbol{A}^{\mathrm{H}}\boldsymbol{P}\boldsymbol{A}\big)^{-1}\boldsymbol{A}^{\mathrm{H}}\boldsymbol{P}\boldsymbol{D}\circ\boldsymbol{I}\Big\}\Big)^{-1}.$$

Thus expression (5), which is a $2 \times 2$ diagonal matrix, can be used to evaluate the quality of the selection, tackling the sensor selection problem. The primary challenges that remain are the binary selection vector $\boldsymbol{p}$, the dependency of the cost on the unknown parameters in $\boldsymbol{\omega}$, the matrix form of the cost, and the relative complexity. To alleviate part of this complexity, we propose to optimize for the worst-case two-target CRB. By fixing the number of targets to two and optimizing for the worst-case over the two targets and over a range of $\boldsymbol{\omega} = [\omega_1, \omega_2]^{\mathrm{T}}$ values, we should obtain an antenna design that is also useful in the multi-target regime. With this, we can formulate our problem of finding an optimal $\boldsymbol{p}$ by combining (4) and (5) into

$$\min_{\boldsymbol{p}\in\{0,1\}^N} \max_{k\in\{1,2\},\boldsymbol{\omega}\in\mathbb{R}^2} [\mathrm{CRB}(\boldsymbol{\omega},\boldsymbol{p})]_{k,k} \quad \text{s.t. } \boldsymbol{1}^{\mathrm{T}}\boldsymbol{p} = M. \quad (6)$$

## 4. TWO-SOURCE CRAMÉR-RAO BOUND SENSOR SELECTION

As we discussed in the previous section, the optimization problem (6) is based on an underlying uniform linear array (ULA). As a result, we have

$$\boldsymbol{a}(\omega_k) = \begin{bmatrix}1 & \mathrm{e}^{\mathrm{j}\omega_k} & \mathrm{e}^{\mathrm{j}2\omega_k} & \cdots & \mathrm{e}^{\mathrm{j}(N-1)\omega_k}\end{bmatrix}^{\mathrm{T}}, \\ \boldsymbol{d}(\omega_k) = \begin{bmatrix}0 & \mathrm{j}\mathrm{e}^{\mathrm{j}\omega_k} & \cdots & \mathrm{j}(N-1)\mathrm{e}^{\mathrm{j}(N-1)\omega_k}\end{bmatrix}^{\mathrm{T}}.$$

To solve (6) we will first do some derivations to simplify the cost function, then we propose a method to handle the worst-case and finally we discuss a convex relaxation of the problem. Before we derive the cost function for each target, let us introduce some notation for convenience:

$$z = \sum_{n=0}^{N-1} p_n, \qquad z(\Delta\omega) = \sum_{n=0}^{N-1} p_n \mathrm{e}^{\mathrm{j}n\Delta\omega}, \qquad (7)$$

$$\bar{z} = \sum_{n=0}^{N-1} p_n n, \qquad \bar{z}(\Delta\omega) = \sum_{n=0}^{N-1} p_n n \mathrm{e}^{\mathrm{j}n\Delta\omega}, \qquad (8)$$

$$\bar{\bar{z}} = \sum_{n=0}^{N-1} p_n n^2, \qquad \boldsymbol{Z}(\Delta\omega) = \begin{bmatrix} z & z(\Delta\omega) \\ z^*(\Delta\omega) & z \end{bmatrix}, \quad (9)$$

$$\bar{\boldsymbol{z}}_1(\Delta\omega) = \begin{bmatrix}\bar{z} \\ \bar{z}^*(\Delta\omega)\end{bmatrix}, \quad \bar{\boldsymbol{z}}_2(\Delta\omega) = \begin{bmatrix}\bar{z}(\Delta\omega) \\ \bar{z}\end{bmatrix}, \qquad (10)$$

where $\Delta\omega = \omega_2 - \omega_1$. Note that all these parameters are linear in $\boldsymbol{p}$. We now define the following cost functions, which are inversely proportional to the diagonal elements of the CRB in (5) in case of two targets:

$$f_k = \boldsymbol{d}^{\mathrm{H}}(\omega_k)\boldsymbol{P}\boldsymbol{d}(\omega_k) - \boldsymbol{d}^{\mathrm{H}}(\omega_k)\boldsymbol{P}\boldsymbol{A}\big(\boldsymbol{A}^{\mathrm{H}}\boldsymbol{P}\boldsymbol{A}\big)^{-1}\boldsymbol{A}^{\mathrm{H}}\boldsymbol{P}\boldsymbol{d}(\omega_k) \\ = \bar{\bar{z}} - \bar{\boldsymbol{z}}_k^{\mathrm{H}}(\Delta\omega)\boldsymbol{Z}^{-1}(\Delta\omega)\bar{\boldsymbol{z}}_k(\Delta\omega). \qquad (11)$$

We observe that the cost functions in (11) only depend on $\Delta\omega$ and no longer on the individual parameters. Furthermore, the cost functions share symmetry:

$$f_1(\Delta\omega) = f_1(-\Delta\omega) = f_2(\Delta\omega) = f_2(-\Delta\omega).$$

This symmetry follows from the equalities $\bar{z}_k(\Delta\omega) = \bar{z}_k^*(-\Delta\omega)$, $\boldsymbol{Z}(\Delta\omega) = \boldsymbol{Z}^*(-\Delta\omega)$, $\bar{z}_1(\Delta\omega) = \boldsymbol{Q}\bar{z}_2^*(\Delta\omega)$ and $\boldsymbol{Z}(\Delta\omega) = \boldsymbol{Q}^{\mathrm{T}}\boldsymbol{Z}^*(\Delta\omega)\boldsymbol{Q}$, where $\boldsymbol{Q}$ is a $2 \times 2$ permutation matrix. Because of the symmetry in the cost functions, we only need to optimize for one of the two and only for positive $\Delta\omega$ values. To handle the worst-case optimization, we propose to grid the possible values of $\Delta\omega$ into a set $\mathcal{D}_+$. This gridding should depend on the possible resolution of the array, which is given by its maximal aperture.

We can now significantly simplify the problem in (6). Using the proposed gridding, $\Delta\omega \in \mathcal{D}_+$, we can optimize the worst-case by applying the following lower bound on the cost in (11):

$$
\begin{aligned}
&\min_{\boldsymbol{p},c} \quad c \\
&\text{s.t.} \quad \mathbf{1}^{\mathrm{T}}\boldsymbol{p} = M, \ \boldsymbol{p} \in \{0,1\}^N \\
&\quad \bar{\bar{z}} - \bar{z}_1^{\mathrm{H}}(\Delta\omega)\boldsymbol{Z}^{-1}(\Delta\omega)\bar{z}_1(\Delta\omega) \geq c^{-1}, \ \forall\Delta\omega \in \mathcal{D}_+.
\end{aligned}
$$

To obtain the final convex optimization problem, we start by applying another bound on the terms that depend on $\Delta\omega$. This leads to

$$
\begin{aligned}
&\min_{\boldsymbol{p},c,g} \quad c \\
&\text{s.t.} \quad \mathbf{1}^{\mathrm{T}}\boldsymbol{p} = M, \ \boldsymbol{p} \in \{0,1\}^N, \ \bar{\bar{z}} - g \geq c^{-1} \\
&\quad \bar{z}_1^{\mathrm{H}}(\Delta\omega)\boldsymbol{Z}^{-1}(\Delta\omega)\bar{z}_1(\Delta\omega) \leq g, \ \forall\Delta\omega \in \mathcal{D}_+.
\end{aligned}
$$

Now we can use the Schur complement on both inequality constraints to obtain two linear matrix inequalities [12], i.e.,

$$
\begin{aligned}
&\min_{\boldsymbol{p},c,g} \quad c \\
&\text{s.t.} \quad \mathbf{1}^{\mathrm{T}}\boldsymbol{p} = M, \ \boldsymbol{p} \in \{0,1\}^N \\
&\quad \begin{bmatrix} \bar{\bar{z}} - g & 1 \\ 1 & c \end{bmatrix} \succeq 0 \\
&\quad \begin{bmatrix} g & \bar{z}_1^{\mathrm{H}}(\Delta\omega) \\ \bar{z}_1(\Delta\omega) & \boldsymbol{Z}(\Delta\omega) \end{bmatrix} \succeq 0, \ \forall\Delta\omega \in \mathcal{D}_+.
\end{aligned}
$$

The above problem, except for the binary vector $\boldsymbol{p}$, is a convex semidefinite program. To obtain the final convex optimization problem, we propose to relax the constraint on $\boldsymbol{p}$ with a box constraint, i.e.,

$$
\begin{aligned}
&\min_{\tilde{\boldsymbol{p}},c,g} \quad c \\
&\text{s.t.} \quad \mathbf{1}^{\mathrm{T}}\tilde{\boldsymbol{p}} = M, \ 0 \leq \tilde{p}_n \leq 1, \ \forall n \in \mathbb{N}^N \\
&\quad \begin{bmatrix} \bar{\bar{z}} - g & 1 \\ 1 & c \end{bmatrix} \succeq 0 \quad\quad\quad (12) \\
&\quad \begin{bmatrix} g & \bar{z}_1^{\mathrm{H}}(\Delta\omega) \\ \bar{z}_1(\Delta\omega) & \boldsymbol{Z}(\Delta\omega) \end{bmatrix} \succeq 0, \ \forall\Delta\omega \in \mathcal{D}_+,
\end{aligned}
$$

and use a rounding procedure in addition to the optimization to obtain the optimal binary values of $\boldsymbol{p}$ from the new continuous vector $\tilde{\boldsymbol{p}}$. For this rounding procedure a randomized rounding scheme [5] can be used to obtain $\boldsymbol{p}$ from $\tilde{\boldsymbol{p}}$. We observe that in many of our simulations the continuous vector $\tilde{\boldsymbol{p}}$ was already very close to being binary and as such, selecting the $M$ largest values of $\tilde{\boldsymbol{p}}$ was often optimal.

**Table 1**. Matched filter output sidelobe levels, relative to the mainlobe level.

| | Average sidelobe level | Worst-case sidelobe level |
|---|---|---|
| $K = 2$ | $-5.39\,\mathrm{dB}$ | $-0.53\,\mathrm{dB}$ |
| $K = 1$ | $-6.07\,\mathrm{dB}$ | $-0.13\,\mathrm{dB}$ |

## 5. SIMULATION RESULTS

To show the effectiveness of our proposed sensor selection method, we present the following simulation results. We compare our method to the single-source method and randomized selection. We set $\mathcal{D}_+$ to be 128 equally spaced numbers between the first null angle and $180°$. The first null angle is approximated by $1.772N^{-1}$, the half-power beamwidth at broadside of a $\frac{\lambda}{2}$-spaced ULA. The single target optimization is given by

$$\min_{\tilde{\boldsymbol{p}}} \ \bar{\bar{z}} - \frac{\bar{z}^2}{M} \quad \text{s.t.} \ \mathbf{1}^{\mathrm{T}}\tilde{\boldsymbol{p}} = M, \ 0 \leq \tilde{p}_n \leq 1, \ \forall n \in \mathbb{N}^N,$$

which will select the $M$ elements closest to the edges of the array.

First, we show some examples of resulting selections, the best selection after 100 rounding attempts. The grids in Fig. 1 each represent a comparison between the single-target and two-target optimization for different values of $N$ and $M$. The first row of each grid represents the single-target optimization result while the second row represents the two-target optimization. We see in Fig. 1 that using the two-target CRBs in the design, we obtain array selections with a mix of edge and center elements. Using the single-target CRB on the other hand results in just edge elements being selected. We have also run simulations with alternative grids $\mathcal{D}_+$. In Fig. 2, we show a selection when $\mathcal{D}_+$ includes fewer small values of $\Delta\omega$, resulting in a selection that is closer to the single-target optimization result. In this case, $\tilde{\boldsymbol{p}}$ has more values further from zero and one and thus, to provide a quality example, we have increased the number of rounding attempts to 1000. When excluding larger values of $\Delta\omega$ from $\mathcal{D}_+$, no notable changes are observed. This suggests that the worst-cases occur for small values of $\Delta\omega$, which makes intuitive sense.

Second, in Fig. 3 we show an example resulting beampattern. While this is not necessarily a fair assessment of the sensor selection, it nevertheless gives insight into the sidelobe pattern and multi-target behavior. In the beampattern design using the two-target CRB we see that there are less sidelobes close to the looking direction compared to the single-target design. Further from the looking direction we see some sidelobes that are larger, but overall it seems there all less lobes in the two-target design, with lobe amplitudes that are more similar to each other compared to the single-target design. To confirm, we have quantified the sidelobe levels of the beampattern in Table 1. As expected, the peak sidelobe for the two-target design is lower than the peak sidelobe of the single-target design, in exchange for slightly higher sidelobes on average. It should be stressed again though, that this is purely for the purpose of a simple illustration, as the matched filter, which is used to generate the beampattern, is known not to reach the multi-target CRB. One may expect more improvement when employing methods that are more appropriate to the multi-target scenario.

Finally, we compare the resulting CRBs for different array sizes with $M = \frac{1}{4}N$ in Fig. 4a and different selection sizes in Fig. 4b. We use here randomized rounding, and the error bands in Fig. 4 indicate the best and worst results of the rounding procedure, while the curves

**Fig. 1**. Array selection results for the single-target and two-target optimizations. From left-to-right then top-to-bottom, $(N, M)$ equals $(128, 32)$, $(64, 16)$, $(32, 8)$, $(16, 4)$, and $(8, 4)$, respectively.
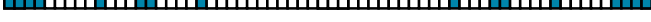


**Fig. 2**. Array selection result for $(N, M) = (64, 16)$, when $\mathcal{D}_+$ is 128 equally spaced points in $[\pi/18, \pi]$.
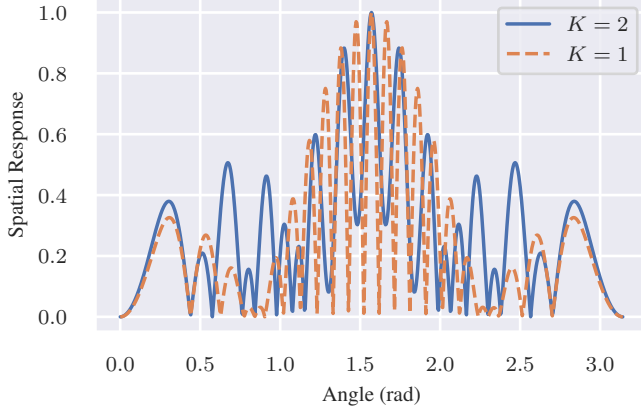


**Fig. 3**. An example beampattern when aiming at broadside for single-target and two-target designs, where $(N, M) = (24, 6)$.

indicate the average. To solve the proposed optimization problem (12) for $\tilde{p}$, we have used the open-source projects CVXPY [13] and CVXOPT [14].[1]
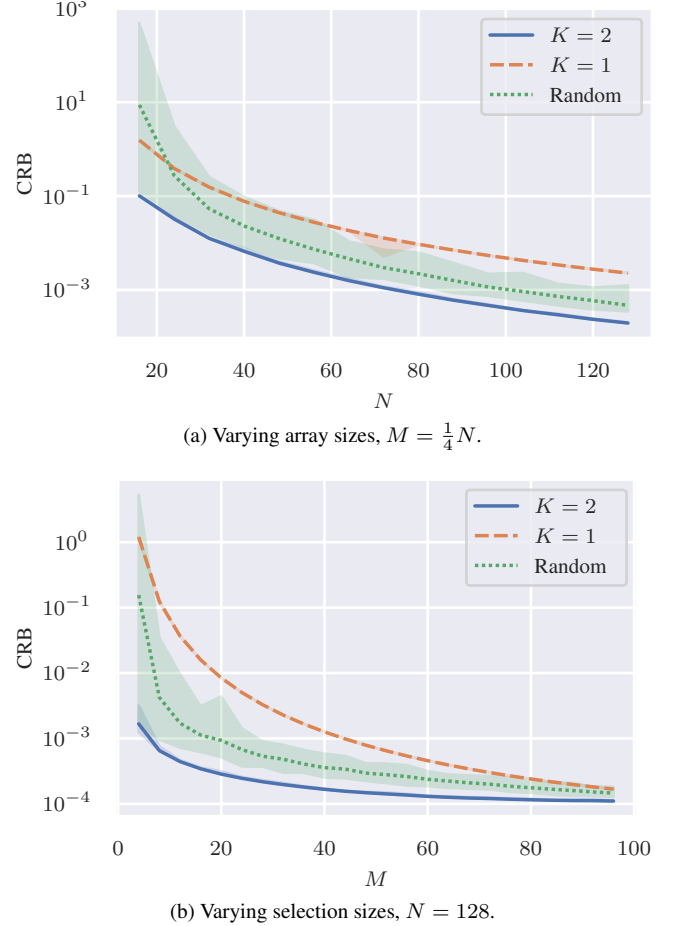
## 6. DISCUSSION

We have presented a method of finding a sensor selection which is optimal in the worst-case two-target CRB. The method is a convex semidefinite program followed by a randomized rounding step and can therefore be efficiently solved [15]. We have shown that using the two-target CRB in the sensor selection problem leads to side-lobe control, without the need for explicit sidelobe suppression constraints in the optimization problem. By adapting the notations in (7) to (10), the method can be applied to non-ULAs.

Through simulation, we have shown that the method outperforms random selection and the sensor selection using the single-target CRB, in terms of the two-target CRB. Finally, the examples of sensor selections that we have shown in Fig. 1 suggest that for the generic ULA, equal power sources scenario, the sensor selection can be optimally done without the need for an explicit optimization.

For future work, we identify a number of interesting avenues. First of all, we currently optimize for the worst-case two-target CRB. Investigating performance when considering instead the average two-target CRB over $\mathcal{D}_+$ may lead to better performance on average, at the risk of occasional performance drops. Second, while a small adjustment to the method overall, quantifying the performance in the non-equal power sources scenario remains to be

[1]A notebook implementing the simulations can be found at https://doi.org/10.5281/zenodo.7716679.



(a) Varying array sizes, $M = \frac{1}{4}N$.



(b) Varying selection sizes, $N = 128$.

**Fig. 4**. Worst-case two-target CRBs for three different selection methods. Lines indicate the average and bands the minimum and maximum values over 100 trials. In these figures $\sigma_e^2/(2T) = 1$.

investigated. We suspect another gridding, similar to $\mathcal{D}_+$, of the unknown relative power difference between the sources, within some bounds, will be helpful in this regard. They can also be considered in a worst-case or average optimization. Third, we could develop the method further to be able to handle correlated sources. We expect the correlated sources scenario to be of particular interest in tracking applications and scenarios with coherent processing intervals that are large enough to allow for prior knowledge on reflectors to be used in the sensor selection problem. This would make the method more applicable to the online sensor selection problem. It should be noted however that the two-target CRB with uncorrelated sources still provides a loose lower bound on the performance in the correlated sources case and may still provide useful results. The investigation into the differences in performance between these two bounds (assuming correlated and uncorrelated sources) remains as well.

# 7. REFERENCES

[1] Joachim H.G. Ender, "On compressive sensing applied to radar," *Signal Processing*, vol. 90, no. 5, pp. 1402–1414, May 2010.

[2] E. Tohidi, M. Radmard, S. M. Karbasi, H. Behroozi, and M. M. Nayebi, "Compressive sensing in MTI processing," in *2015 3rd International Workshop on Compressed Sensing Theory and Its Applications to Radar, Sonar and Remote Sensing (CoSeRa)*, June 2015, pp. 189–193.

[3] Kumar Vijay Mishra and Yonina C. Eldar, "Sub-Nyquist Radar: Principles and Prototypes," in *Compressed Sensing in Radar Signal Processing*, Antonio De Maio, Yonina C. Eldar, and Alexander M. Haimovich, Eds., pp. 1–48. Cambridge University Press, first edition, Sept. 2019.

[4] Siddharth Joshi and Stephen Boyd, "Sensor Selection via Convex Optimization," *IEEE Transactions on Signal Processing*, vol. 57, no. 2, pp. 451–462, Feb. 2009.

[5] Sundeep Prabhakar Chepuri and Geert Leus, "Sparsity-Promoting Sensor Selection for Non-Linear Measurement Models," *IEEE Transactions on Signal Processing*, vol. 63, no. 3, pp. 684–698, Feb. 2015.

[6] Saeid Sedighi, Bhavani Shankar, Mojtaba Soltanalian, and Bjorn Ottersten, "One-Bit DoA Estimation via Sparse Linear Arrays," in *ICASSP 2020 - 2020 IEEE International Conference on Acoustics, Speech and Signal Processing (ICASSP)*, Barcelona, Spain, May 2020, pp. 9135–9139, IEEE.

[7] Hana Godrich, Athina P. Petropulu, and H. Vincent Poor, "Sensor Selection in Distributed Multiple-Radar Architectures for Localization: A Knapsack Problem Formulation," *IEEE Trans. Signal Process.*, vol. 60, no. 1, pp. 247–260, Jan. 2012.

[8] Venkat Roy, Sundeep Prabhakar Chepuri, and Geert Leus, "Sparsity-enforcing sensor selection for DOA estimation," in *2013 5th IEEE International Workshop on Computational Advances in Multi-Sensor Adaptive Processing (CAMSAP)*, St. Martin, France, Dec. 2013, pp. 340–343, IEEE.

[9] Ehsan Tohidi, Mario Coutino, Sundeep Prabhakar Chepuri, Hamid Behroozi, Mohammad Mahdi Nayebi, and Geert Leus, "Sparse Antenna and Pulse Placement for Colocated MIMO Radar," *IEEE Trans. Signal Process.*, vol. 67, no. 3, pp. 579–593, Feb. 2019.

[10] P. Stoica and Arye Nehorai, "MUSIC, maximum likelihood, and Cramer-Rao bound," *IEEE Transactions on Acoustics, Speech, and Signal Processing*, vol. 37, no. 5, pp. 720–741, May 1989.

[11] A.B. Gershman and J.F. Bohme, "A note on most favorable array geometries for DOA estimation and array interpolation," *IEEE Signal Process. Lett.*, vol. 4, no. 8, pp. 232–235, Aug. 1997.

[12] Stephen P. Boyd and Lieven Vandenberghe, *Convex Optimization*, Cambridge University Press, Cambridge, UK ; New York, 2004.

[13] Steven Diamond and Stephen Boyd, "CVXPY: A Python-embedded modeling language for convex optimization," *Journal of Machine Learning Research*, vol. 17, no. 83, pp. 1–5, 2016.

[14] Martin Andersen and Lieven Vandenberghe, "CVXOPT: Python software for convex optimization," 2022, [Online]. Available: https://cvxopt.org. [Accessed: 14- Oct- 2022].

[15] Lieven Vandenberghe and Stephen Boyd, "Semidefinite Programming," *SIAM Rev.*, vol. 38, no. 1, pp. 49–95, Mar. 1996.